Desalination and Water Treatment
www.deswater.com

doi: 10.1080/19443994.2015.1090915

57 (2016) 18182–18193
August

Taylor & Francis
Taylor & Francis Group

Removal of an azo dye (Alizarin yellow) in homogeneous medium using direct photolysis, acetone/UV, H_2O_2/UV, $S_2O_8^{2-}$/UV, H_2O_2/$S_2O_8^{2-}$/UV, and $S_2O_8^{2-}$/heat

S. Aliouche, K. Djebbar*, T. Sehili

Laboratory of Science and Technology of Environment, Department of Chemistry, University Mentouri Constantine, Constantine, Algeria, Tel. +213 0 5 53 00 44 85; email: alsihame@yahoo.fr (S. Aliouche), Tel. +213 0 7 74 82 17 17; email: kedjebbar@yahoo.fr (K. Djebbar), Tel. +213 0 7 70 74 01 36; email: tsehili@yahoo.fr (T. Sehili)

Received 26 January 2015; Accepted 29 August 2015

ABSTRACT

The azo dyes are considered as one of the highest toxic compounds of water pollution. Decolorization of these compounds has been carried out via photochemical methods (direct UV photolysis and advanced oxidation processes abbreviated as AOPs) since they are highly resistant to conventional treatment. In this study, direct UV photolysis (under 254, 365, 310 nm, and solar), acetone/UV (254 nm and acetone as a sensitizer), H_2O_2/UV, $S_2O_8^{2-}$/UV, $S_2O_8^{2-}$/H_2O_2/UV and $S_2O_8^{2-}$/heat (absence of light), have been investigated in lab-scale experiments for decolorization of Alizarin yellow (abbreviated as AY). From the experimental results, it has been found that color removal followed the increasing order: UV photolysis (negligible) < acetone/UV < $S_2O_8^{2-}$/heat < $S_2O_8^{2-}$/H_2O_2/UV < $S_2O_8^{2-}$/UV < H_2O_2/UV. This improvement might be attributed strictly to radicals $HO^{\cdot}$ in the case of H_2O_2/UV, $HO^{\cdot}$ and $SO_4^{\cdot-}$ in the case of $S_2O_8^{2-}$/UV, and heat/$S_2O_8^{2-}$ in absence of light. The effects of parameters like concentrations of H_2O_2, $S_2O_8^{2-}$ and acetone, and temperature have been studied and the optimum operational conditions were found. In another part, the UV–Vis spectral changes of AY during UV/H_2O_2 and UV/$S_2O_8^{2-}$ treatments, showed that it was easier to destroy the bonding linkage –N=N– and then the long chain C=C (bathochromic system). Decolorization kinetic followed the pseudo-first-order for all systems.

Keywords: Alizarin yellow; UV; Solar irradiation; Photolysis; H_2O_2; $S_2O_8^{2-}$; Advanced oxidation processes; Temperature

1. Introduction

The discharge of effluents from the textile dyeing and finishing industries in rivers is considered as an important source of environmental contamination. Indeed, the azo dyes are toxic [1], resistant to biodegradation [2] due to their complex aromatic structure, and they can transform into carcinogenic compounds [3–6]. Several approaches were undertaken in order to reduce or to eliminate these hazardous substances: ions exchange [7,8], flocculation [9], coagulation [10], adsorption on various supports [11], biological treatment [12], etc. Unfortunately, most of these conventional methods were ineffective, very expensive, and

---

*Corresponding author.

may often produce secondary pollution by the transfer of the pollutants from one phase to another like adsorption [13]. Consequently, advanced oxidation processes (abbreviated AOPs) are alternative and innovative options for the treatment of the textile wastewater. They can destroy or reduce to a very feeble level recalcitrant substance [14]. The effectiveness of these AOPs is related to the productions of very reactive species: the hydroxyl radicals. Indeed, once produced from the photolysis of H_2O_2 at 254 nm and according to their high oxidation potential (2.9 V; [15]), they may react rapidly (with a high rate constant of $10^{10}\ M^{-1}\ s^{-1}$) and without any specificity with a broad range of organic compounds [16]. In addition, the bleaching process may occur via radicals $SO_4^{\bullet -}$ produced from photolysis of $S_2O_8^{2-}$ at 254 nm or from heat in absence of light. Having a high oxidation potential (2.8 V), the $SO_4^{\bullet -}$ can oxidize many organic compounds but with more selectivity compared to radicals $HO^{\bullet}$ [15]. Similar studies conducted by H_2O_2/UV and $S_2O_8^{2-}$/UV systems have been related in the literature [17,18].

The aim of this research is to evaluate and to compare the effectiveness of some photochemical systems such as direct UV photolysis, UV/acetone (acetone acting as photosensitizer), $S_2O_8^{2-}$/UV, H_2O_2/UV, $H_2O_2/S_2O_8^{2-}$/UV, and $S_2O_8^{2-}$/heat (in absence of light) on the depletion of an azo dye, Alizarin yellow. The influence of H_2O_2 and $S_2O_8^{2-}$ concentration, pH, concentration of AY, and temperature were investigated. The optimal operational conditions were examined. The UV–vis spectral changes of AY during H_2O_2/UV and $S_2O_8^{2-}$/UV treatment processes will be examined.

2. Experimental

2.1. Materials

AY was furnished from Fluka chemical company and was used as received. Hydrogen peroxide (H_2O_2 30%, Fluka), potassium persulfate ($K_2S_2O_8$ 99%, Aldrich), and acetone (C_3H_6O d = 0.79, Labosi) solutions were prepared with ultrapure water from a Milli pure water (Milli-Q purification unit). The pH of the solutions was adjusted with NaOH or HCl (supplied both by Labosi) to attain desired values (pH 1.7, pH 2, pH 11.5, and pH 12). The structure of AY took at 1.6×10^{-4} M and in its natural pH (5.6), is represented in Fig. 1.

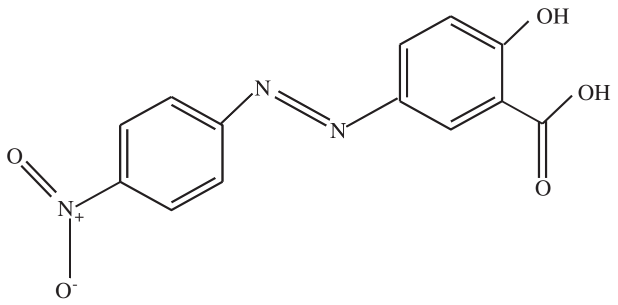

Fig. 1. Structure of Alizarin yellow.

2.2. Description of the used photoreactors

Irradiation experiments were performed at 254 nm in a cylindrical reactor in quartz (100 cm of length and 2 cm in diameter) located on one of the principal axes of the assembly and equipped with three symmetrical externals low-pressure mercury lamps (germicide lamp, Philips TUV 15 W) emitting principally at 254 nm. The reactor is surrounded symmetrically by these lamps. The temperature is maintained between 18°C and 20°C using an airflow provided by a ventilator. The whole system is placed in a cylindrical enclosure [19].

In solar light, aqueous solutions of the dye are degraded by direct photolysis and by H_2O_2/UV using a pilot plant containing a reservoir delivery, a pump, and an assembly of tubes on Pyrex. They are located closely to each other toward natural light. Samples are withdrawn at regular time intervals and analyzed immediately [20] (Fig. 2).

2.3. Analyses

The UV–vis spectra of the dye were recorded from 200 to 800 nm using a UV–Vis spectrophotometer "Helios α-Unicam Spectronic." The maximum wavelength absorbance (λ_{max}) of AY was located at 428 nm from the spectra. Thus, the residual concentration of the dye in the reaction mixture at different reaction times was calculated by measuring the absorption intensity at $\lambda_{max} = 428$ nm from a calibration curve. The efficiency of color removal was expressed from the following relation [21]:

$$\text{Efficiency}\ (\%) = \left(1 - \frac{C_t}{C_0}\right) \times 100 \quad (1)$$

where C_0 is the initial concentration of AY and C_t is the concentration of the substrate at reaction time t.

3. Results and discussion

3.1. UV–vis spectrum of AY

The UV–vis spectrum of AY in natural pH (5.6) and in dilute concentration (1.6×10^{-4} M) shows that this compound exhibits an intense band located

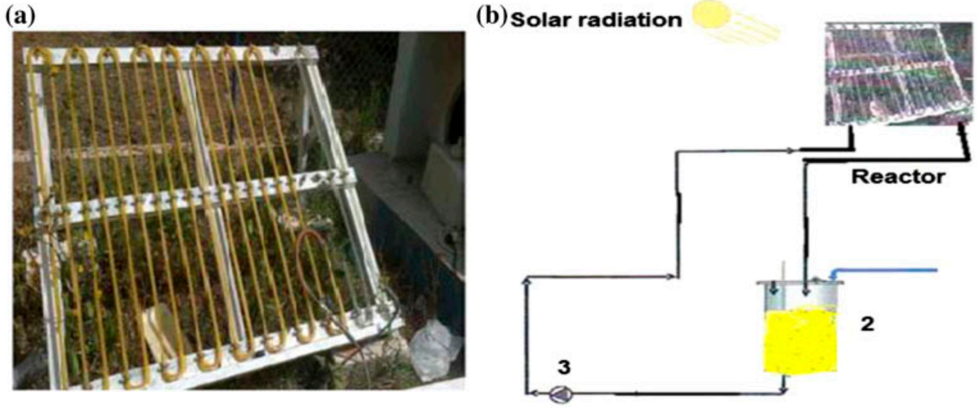

Fig. 2. Setup of pilot plant solar light: (a) the solar reactor and (b) scheme of the device.
Notes: (1) tube on Pyrex, (2) dye solution and H_2O_2 reservoir delivery, and (3) pump.

around 257 nm (UV region, with a molar absorption coefficient equal to 19,537 M^{-1} cm^{-1}) and a less intense one at around 428 nm (visible region, with a molar absorption coefficient equal to 3,735 M^{-1} cm^{-1}).

The pH affected the behavior of the substrate, mainly in basic medium (pH 12). Indeed, we observe a color change of the solution (turning into red) and a shift of the latter band (100 nm) involving thus a bathochromic effect. This color change can be due to the deprotonation process. Besides, we observe the apparition of a new band at 334 nm related to the naphthalene ring. By contrast, we remark no change in color and also in band positions in acidic medium ($pH \leq 2$) (Fig. 3).

3.2. UV direct photolysis (254 nm) of AY

3.2.1. Effect of the initial AY concentration

This process is applied to degrade AY in dilute (1.6×10^{-4} M) and aerated medium. The photolysis is carried out in a static tubular reactor under artificial UV irradiation at 254 nm and monitored by a spectrophotometer. The obtained results show that this compound does not undergo photolysis: 4.5% (1.6×10^{-4} M), 5.43% (1.3×10^{-4} M), and 6.1% (9.7×10^{-5} M) (Fig. 4(a)). This can be attributed to the molecule size present in the solution, preventing the exposure of certain of them to the photons and also to the absence of powerful oxidants (like $HO^{\bullet}$) which may destroy the molecule [22]. This fact is also related to the very weak quantum yield of the substrate (no absorption of light). Other experiments are achieved under 310 and 365 nm in artificial light. The obtained results indicate that the efficiency of color removal is not significant too (Fig. 4(b)). This fact can be attributed to the weakness of both the energy sources. In solar light, same results are obtained due to the weak participation of photons issued from this source. Indeed, solar radiation reaching the surface of the earth has a feeble energy ($\lambda \geq 380$ nm, Fig. 4(b)).

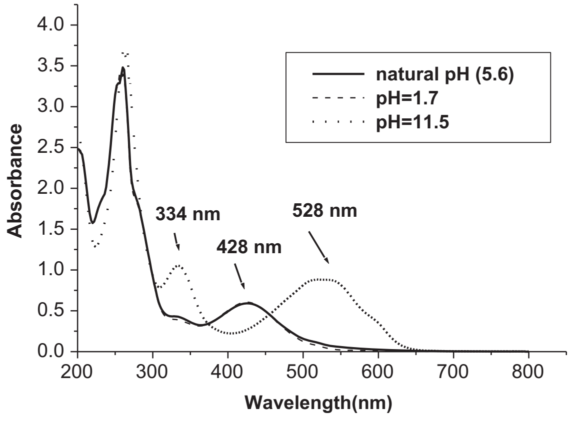

Fig. 3. Spectrum of AY (1.6×10^{-4} M). Influence of pH.

3.3. Photo-oxidation process of AY

3.3.1. Sensitivity of AY in the presence of acetone, H_2O_2, and $S_2O_8^{2-}$ in the absence of light

Before studying the decolorization process of AY by acetone/UV, H_2O_2/UV, and $S_2O_8^{2-}$/UV, it is necessary to check if oxidation reaction may occur between the substrate and the acetone, the hydrogen peroxide, and the persulfate in dark conditions. The obtained results show that AY is not sensitive toward H_2O_2, $S_2O_8^{2-}$, and acetone for their highest concentration: 10^{-1} M.

3.4. Acetone/UV process

Previous studies conducted on photolysis at different wavelengths (254, 365, and 310 nm even in solar light) are ineffective. Thus, to enhance the color removal of this dye, we used acetone as sensitizer in the presence of artificial light (254 nm) [23]. Indeed, when acetone is irradiated with UV light, it can lead to a triplet state (acetone*) characterized by a high energy: 79–82 kcal/mol. Thus, after excitation, a collision between molecules of AY and the excited state of acetone will generate an energy transfer, and will accelerate the process of decolorization of the substrate, mainly at the highest concentration of the sensitizer [23,24]:

$$\text{Acetone} + h\upsilon \rightarrow \text{Acetone}^{*} \tag{2}$$

$$\text{Dye} + \text{Acetone}^{*} \rightarrow \text{Dye}^{*} + \text{Acetone} \tag{3}$$

$$\text{Dye}^{*} \rightarrow \text{Decolorization} \tag{4}$$

According to Eq. (3), we notice an energy transfer and a total regeneration of the acetone.

The entire elimination of the dye is explained by Eq. (4) and reported in Fig. 5.

Kinetic results of AY with the different initial acetone concentrations (10^{-1}, 10^{-2}, and 10^{-3} M) in the presence of acetone/UV process are shown in Fig. 6(a). We observe that:

(1) The presence of acetone acting as a sensitizer increases the rate constant of decolorization.
(2) The removal efficiency (expressed in %) increases as the concentration of acetone increases.

Furthermore, the disappearance of the dye can be described by a pseudo-first-order kinetics (Fig. 6(b)):

$$-\frac{dC}{dt} = k_{\text{app}}C \tag{5}$$

The integration of this expression yields the following result:

$$\ln\left(\frac{C_0}{C}\right) = kt \tag{6}$$

The slope of the plot of $\ln C_0/C$ vs. time gives k_{app} values which are deduced graphically under our experimental conditions.

Under these conditions, the value of R^2 which is above 0.97, shows that color removal of AY using acetone/UV process, follows the pseudo-first-order kinetic model for concentrations of acetone equal to 10^{-2} and 10^{-1} M. The rate efficiency (expressed in %), k_{app}, and values of R^2 are listed in Table 1.

3.5. Photo-oxidation process by H_2O_2/UV

3.5.1. Effect of the concentration of H_2O_2 (artificial light)

The direct photolysis under different wavelengths and solar light is not significant. The same results are obtained in the presence of H_2O_2 in the dark. However, when H_2O_2 is combined with UV irradiation, mainly at 254 nm, we observe a drastic increase in bleaching rate of the process. This effect is attributed to the participation of radicals $HO^{\bullet}$ produced from the photolysis of H_2O_2 (breaking of the O–O bond). These radicals are able to react with a broad range of organic compounds with a rate constant: 10^{10} M^{-1} s^{-1} [12]. Moreover, the rate of degradation increases with increasing concentration of H_2O_2 under some experimental conditions: fixed concentration of AY (1.6×10^{-4} M), various concentrations of H_2O_2 (10^{-3} M, 10^{-2} M, 2×10^{-2} M, and 10^{-1} M), and natural pH (4.9). Indeed, the results reported in Fig. 7(a), show that the

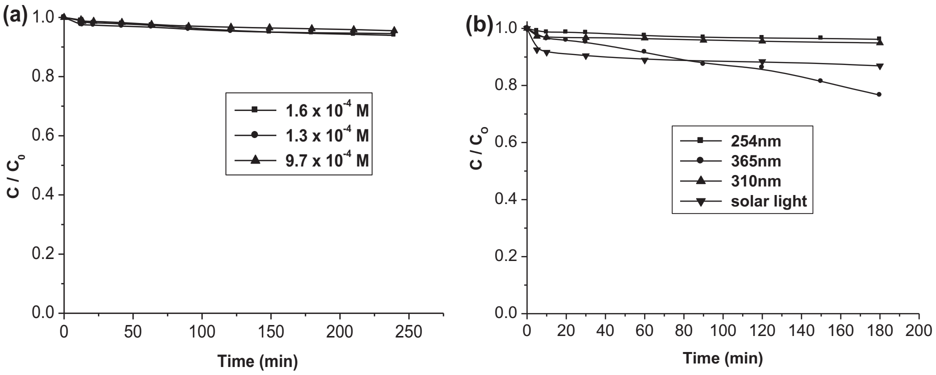

Fig. 4. Decolorization of AY by direct UV photolysis: (a) influence of initial concentration and (b) direct UV photolysis of AY (1.6×10^{-4} M) under 254, 365, 310 nm, and solar light.

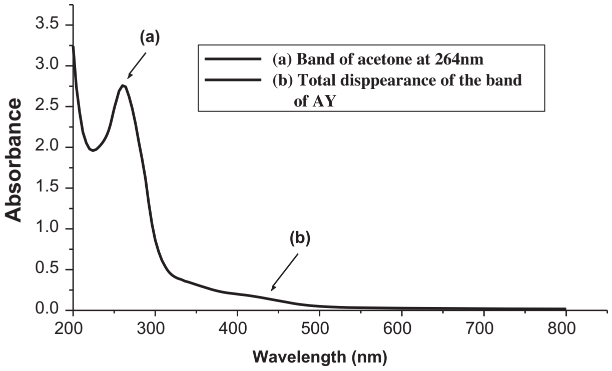

Fig. 5. Absorption spectrum at the end of the degradation reaction of AY (1.6×10^{-4} M) by acetone (10^{-1} M)/UV process. Irradiation time = 120 min.

bleaching process is much reduced comparatively to that obtained with acetone/UV: 99.17% for a reaction time of 35 min for H_2O_2/UV and 92.31% for a reaction time of 240 min for acetone/UV. However, for the highest concentration of H_2O_2 (2×10^{-1} M), we observe a slight decrease in the elimination rate of the dye, suggesting a scavenger effect of H_2O_2 toward the powerful hydroxyl radicals [25–28]:

$$H_2O_2 + HO^\cdot \rightarrow HO_2^\cdot + H_2O \quad k_{H_2O_2} = 2.7 \times 10^7\ M^{-1}\ s^{-1} \tag{7}$$

$$HO^\cdot + HO_2^\cdot \rightarrow H_2O + O_2 \tag{8}$$

3.5.2. Kinetic behavior

The decolorization process may be expressed by the following relation [13]:

$$-\frac{dC_{AY}}{d}t = k_1 C_{AY} C_{HO^\cdot} + K_2 C_{AY} C_{HO_2^\cdot} \tag{9}$$

where C_{AY}, $C_{HO^\cdot}$, and $C_{HO_2^\cdot}$ represent substrate, hydroxyl radical, and peroxyl radical concentrations, respectively. Furthermore, we consider that hydroxyl and peroxyl radicals are constant because they reach the equilibrium state rapidly (process of steady state). Additionally, the oxidation potential of $HO_2^\cdot$ is inferior to that of $HO^\cdot$ and then, it can be neglected. Therefore, the expression rate of the above Eq. (9) may be reduced to a simple kinetic model:

$$-\frac{dC}{dt} = k_{app} C \tag{10}$$

The integration of Eq. (10) conducts to the final expression:

$$\ln\left(\frac{C_0}{C}\right) = k_{app} t \tag{11}$$

where C_0 is the initial concentration of the substrate, C the concentration at instant t, and k_{app} is the pseudo-first-order kinetic constant. The apparent rate constants of H_2O_2/UV process are deduced by plotting $\ln(C_0/C)$ vs. time. The straight lines obtained confirm the reasonable choice of the pseudo-first-order kinetic model (Fig. 7(b)). One observes that only the curves corresponding to the concentration of H_2O_2 equal to 2×10^{-1} and 10^{-1} M have a pseudo-exponential shape (insert in Fig. 7(a)); corresponding to the pseudo-first-order kinetic behavior ($R^2 > 0.96$). However, we notice that for the highest concentration in H_2O_2, the rate constant decreases. This observation can be attributed to the scavenging effect of $HO^\cdot$. All parameters describing the process such as efficiency, R^2, and apparent rate constant are summarized in Table 2.

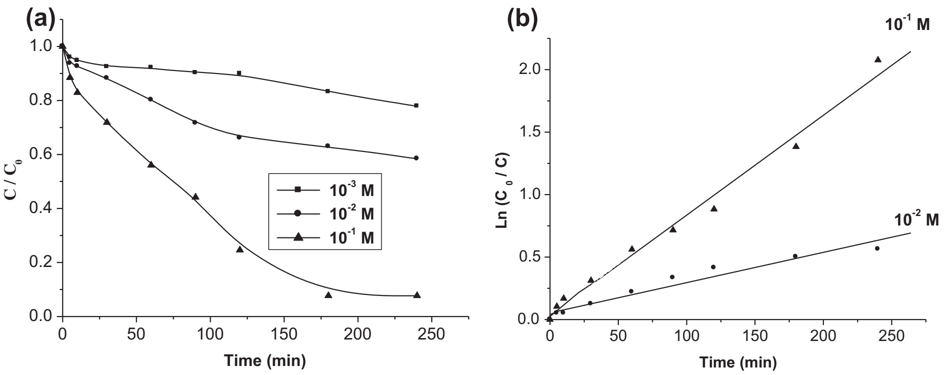

Fig. 6. Decolorization of the dye (1.6×10^{-4} M) by acetone/UV process, λ_{irr} = 254 nm: (a) Effect of acetone concentration in the AY degradation and (b) pseudo-first-order plot of degradation of the dye.

Table 1
Values of pseudo-first-order kinetics constants (k_{app}), rate percent (obtained for a reaction time of 240 min), and R^2 of dye degradation by acetone/UV process at 254 nm

C_0 (M)	Rate (%)	R^2	Apparent rate constants (min^{-1})
10^{-3}	25.86	–	–
10^{-2}	41.60	0.97353	2.42×10^{-3}
10^{-1}	92.31	0.99378	7.99×10^{-3}

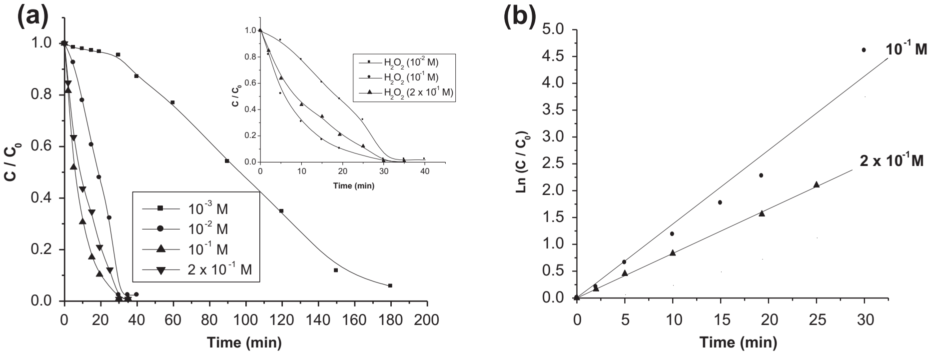

Fig. 7. Decolorization process of AY (1.6×10^{-4} M) by H_2O_2/UV: (a) Effect of H_2O_2 concentration and (b) first-order plot of color degradation of AY solutions as a function of UV irradiation time: pH 4.9, λ_{irr} = 254 nm.

3.5.3. Spectral evolution of AY by H_2O_2/UV

The changes in the absorption spectra of the AY during the H_2O_2/UV process at different reaction times are displayed in Fig. 8. We notice that peaks located at 257 nm in the UV region (ascribed essentially to the absorption of the π–π^* transition of aromatic ring) and at 428 nm in the visible region (ascribed to the absorption of the n–π^* transition and related to the lone pair of electrons belonging to the –N=N– and C=O groups) disappeared in 180, 40, and 30 min for H_2O_2 concentrations equal to 10^{-3}, 10^{-2}, and 10^{-1} M, respectively. However, the UV band at 257 nm decreases at lower rate comparatively to the visible band, showing thereby the destruction of aromatic ring which is often difficult to destroy. We may conclude that the bleaching process is attributed to the attack of the azo group with an opening of the –N=N– bond by radical HO· followed by the entire destruction of the π conjugated system [29].

3.5.4. H_2O_2/UV in solar light

The results reported in Fig. 9 show that the rate of decolorization in solar light was much lower than the one obtained in artificial light. This fact might be explained by a negligible production of radicals HO·. Indeed, the minor inclusion of the UV in natural light (almost 5%, at 290 nm) provides a very feeble energy to break the O–O bond. So, the energy obtained at 380 nm, which is the solar radiation reaching the

Table 2
Values of pseudo-first-order kinetics constants (k_{app}), rate percent (for a reaction time of 30–40 min), and R^2 of dye degradation by H_2O_2/UV process at 254 nm

C_0 (M)	Rate (%)	R^2	Apparent rate constants (min^{-1})
10^{-3}	13.02	–	–
10^{-2}	97.68	–	–
10^{-1}	99.17	0.98595	0.13775
2×10^{-1}	98	0.96467	0.08304

surface of the earth, is not able to produce a large amount of these radicals $HO^{\cdot}$.

Nevertheless, a slow decolorization process is observed beyond 50 min during the dye exposure to the solar light. Accordingly, the rate efficiency is equal to 68% for a reaction time of 240 min.

3.6. Phototransformation of AY by $S_2O_8^{2-}$/UV process at 254 nm

3.6.1. $S_2O_8^{2-}$/UV process

Persulfate is a powerful oxidant ($E_0 = 2.1$ eV) and is relatively stable during storing and treatment [30], and can generate free sulfate radicals ($SO_4^{\cdot -}$) under activation condition of heating [31–34] or UV light [14,21,35,36].

The obtained radical represents a broad absorption band between 300 and 600 nm with a maximum at 455 nm and a molar absorption coefficient of about 1,600 M^{-1} cm^{-1} [37].

Like hydrogen peroxide, the absorption of photons by $S_2O_8^{2-}$ causes the rupture of the peroxide bond to give birth to two sulfate radical anions:

$$S_2O_8^{2-} + h\upsilon \rightarrow 2SO_4^{\cdot -} \qquad (12)$$

The radical anion is a powerful oxidant; and is therefore capable of oxidizing most organic compounds. It may also remove an electron from a molecule in H_2O to give a hydroxyl radical:

$$SO_4^{\cdot -} + H_2O \rightarrow HSO_4^{-} + HO^{\cdot} \qquad (13)$$

From these relationships, it is clear that radicals $SO_4^{\cdot -}$ and $HO^{\cdot}$ participate in the oxidation process of the substrate.

3.6.2. Effect of initial $S_2O_8^{2-}$ concentration

The effect of initial persulfate concentration on photo-oxidation of AY at natural pH (5) is reported in Fig. 10(a). We observe that the efficiency increases as the initial concentration in $S_2O_8^{2-}$ is increased. The removal rate is practically equal to 100% for a reaction time of 40 min under UV-254 nm/$S_2O_8^{2-}$ process and with the highest concentration of persulfate (10^{-1} M). This performance may be attributed to the complete reaction of $SO_4^{\cdot -}$. However, a probable contribution of radicals $HO^{\cdot}$ may occur according to (Eq. 13) and making thus the decolorization process more rapid. By contrast, when concentration in $S_2O_8^{2-}$ is equal to

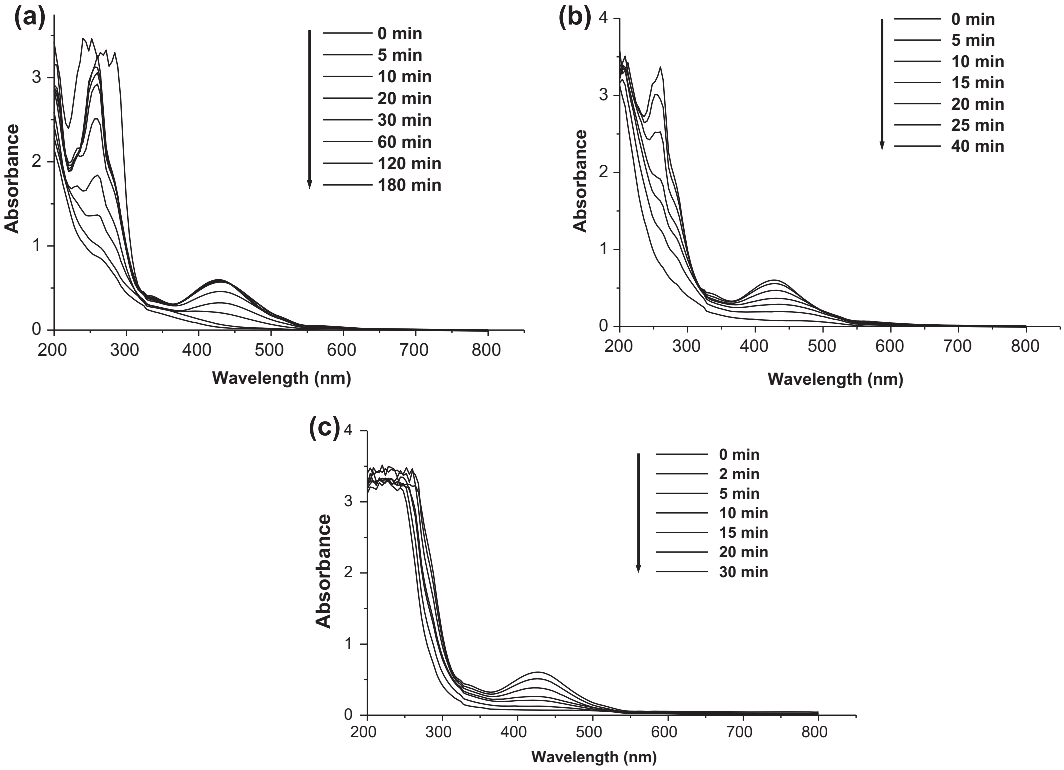

Fig. 8. Spectral evolution of the bleaching process of AY (1.6×10^{-4} M) by H_2O_2/UV at different concentrations: (a) 10^{-3} M, (b) 10^{-2} M, and (c) 10^{-1} M.

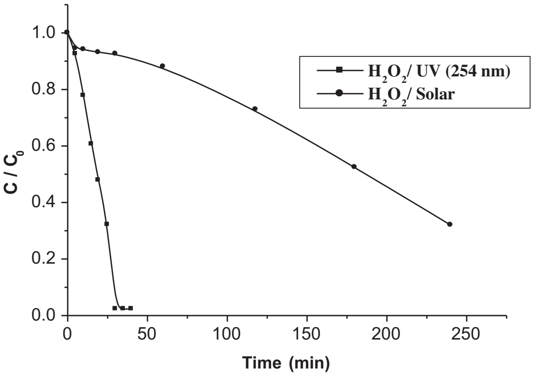

Fig. 9. Effect of light on the docolorization process of AY (1.6×10^{-4} M) in presence of H_2O_2 (10^{-2} M)/UV at 254 nm and H_2O_2 (10^{-2} M)/solar.

10^{-3} M (the lowest one), efficiency value was found feeble: about 30% for a reaction time of 150 min.

Moreover, the decolorization of AY by $S_2O_8^{2-}$/UV follows a pseudo-first-order kinetic model for the concentration in $S_2O_8^{2-}$ equal to 10^{-1} and 10^{-2} M:

$$\ln\left(\frac{C_0}{C}\right) = kt \qquad (14)$$

We notice that the k values increased as the concentration of $S_2O_8^{2-}$ increases (Fig. 10(b)). Thus, slope of plot of $\ln C_0/C$ vs. time, which gives these k values with a correlation coefficient R^2 above 0.96, confirms that this degradation is well described by pseudo-first-order kinetic model (Table 3).

As with H_2O_2/UV, the spectral evolution obtained in $S_2O_8^{2-}$/UV system shows that decolorization process is characterized by a rapid destruction of bands in the visible (n–π^* transitions related also to the lone pair of electrons belonging to the C=O and –N=N– groups of the dye) and in the ultraviolet region (π–π^* transitions of the benzene rings) (Fig. 11).

3.6.3. Effect of the initial pH

The pH effect on the decolorization of AY by $S_2O_8^{2-}$/UV is depicted in Fig. 12. We find that the decolorization performance increases with the augmentation of pH. This is likely due to the concentration effect of active radicals in the solution. Moreover, in acidic medium (pH 2), this process is slightly slower than that obtained at natural pH. This is due to the less reactivity of sulfate radical toward the dye. At pH 12, the decrease in dye concentration (data not shown) cannot be related only to the production of $HO^\bullet$ (Eq. (15)) as the dye structure changes (Fig. 3):

$$SO_4^{\bullet-} + OH^- \rightarrow SO_4^{2-} + HO^\bullet \qquad (15)$$

Consequently, it is not possible to make a comparison with the results obtained in acidic and in neutral media.

3.7. $S_2O_8^{2-}/H_2O_2/UV$ process

A set of experiments are achieved to investigate the decolorization of the substrate by $S_2O_8^{2-}/H_2O_2$/UV system. Indeed, simultaneous addition of $S_2O_8^{2-}$ and H_2O_2, both taken at same concentrations (10^{-2} M) and under UV irradiation (254 nm), gives a slight decrease in the dye comparatively to that obtained with H_2O_2/UV and $S_2O_8^{2-}$/UV separately (Fig. 13). The percentages of degradation by H_2O_2/UV, $S_2O_8^{2-}$/UV, and $S_2O_8^{2-}/H_2O_2$/UV are, respectively, 97.68, 81.37, and 60% for a reaction time of 40 min. This feature may be explained, in one part by a competition of the emitted light between H_2O_2 and $S_2O_8^{2-}$

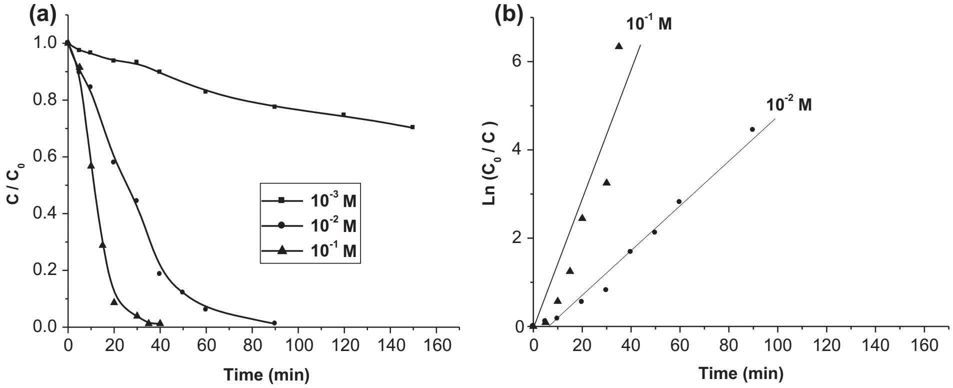

Fig. 10. Decolorization process of AY (1.6×10^{-4} M) by $S_2O_8^{2-}$/UV: (a) in the presence of different concentrations of $S_2O_8^{2-}$ and (b) kinetics of AY decolorization by $S_2O_8^{2-}$/UV process. pH 5, λ_{irr} = 254 nm.

Table 3
Values of pseudo-first-order kinetics constants (k_{app}), rate percent (for a reaction time of 40 min), and R^2 of dye degradation by $S_2O_8^{2-}$/UV process at 254 nm

C_0 (M)	Rate (%)	R^2	Apparent rate constants (min^{-1})
10^{-3}	10.31	–	–
10^{-2}	81.37	0.98990	5.07×10^{-3}
10^{-1}	98.76	0.96079	17.24×10^{-3}

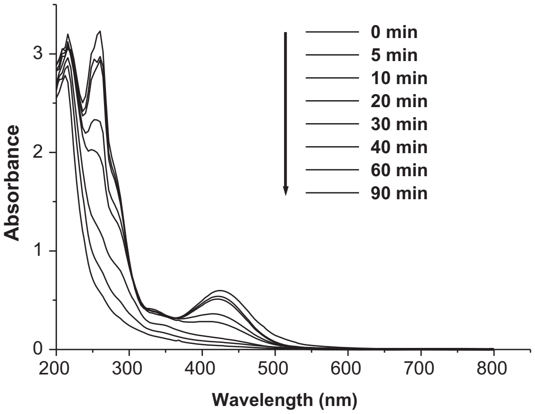

Fig. 11. Spectral evolution of AY (1.6×10^{-4} M) by $S_2O_8^{2-}$ (10^{-2} M)/UV.

which may slow down the production of the two radicals and in another part by a difference of reactivity of $HO^{\bullet}$ (occurring without discrimination) and $SO_4^{\bullet-}$ (occurring with a great selectivity).

3.8. $S_2O_8^{2-}$/heat

3.8.1. Effect of the temperature on the decolorization process of AY by $S_2O_8^{2-}$/heat

It is possible to produce sulfate radical anions in absence of light and using the temperature [18]. This method has been widely studied and has been considered to be very effective [23]. This feature is based on the cleavage of O–O bond to produce $SO_4^{\bullet-}$ at relatively high temperature:

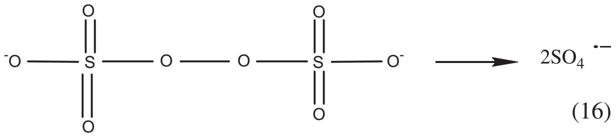

$$^{-}O-S(=O)_2-O-O-S(=O)_2-O^{-} \longrightarrow 2SO_4^{\bullet-} \quad (16)$$

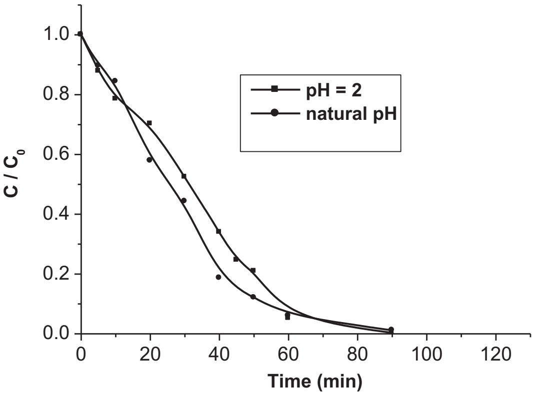

Fig. 12. Effect of initial pH on the decolorization of AY (1.6×10^{-4} M) by $S_2O_8^{2-}$ (10^{-2} M)/UV.

By referring to Fig. 14, we observe that the reaction rate of $SO_4^{\bullet-}$ with the substrate was negligible at an ambient temperature (20˚C) and also at 30˚C. Thus, this result can be attributed to the uncatalyzed decomposition reaction of persulfate, revealing therefore a non-cleavage of the O–O bond. By contrast, when persulfate is heated at 40˚C, the substrate is first decolorized at about 60% for a reaction time of 180 min. Furthermore, the efficiency rate reaches 100% at 50 and 60˚C for reaction time of 160 and 110 min, respectively.

Once sulfate radicals are produced by heat, they may react with the dye via a series of radical chain reactions, showing thus, the bleaching process of the dye (Eqs. (17)–(25)) [37,38]:

$$S_2O_8^{2-} \xrightarrow{\text{Heat}} 2SO_4^{\bullet-} \quad (17)$$

$$SO_4^{\bullet-} + H_2O \Leftrightarrow HO^{\bullet} + HSO_4^{-} \qquad k = 9.4 \times 10^3\ s^{-1} \quad (18)$$

$$SO_4^{\bullet-} + Dye \rightarrow Dye^{\bullet} + Products \quad (19)$$

$$HO^{\bullet} + Dye \rightarrow Dye^{\bullet} + Products \quad (20)$$

$$Dye^{\bullet} + S_2O_8^{2-} \rightarrow SO_4^{\bullet-} + Products \quad (21)$$

$$SO_4^{\bullet-} + HO^{\bullet} \rightarrow Chain\ termination \quad (22)$$

$$2HO^{\bullet} \rightarrow Chain\ termination \qquad k = 5 \times 10^9\ M^{-1}\ s^{-1} \quad (23)$$

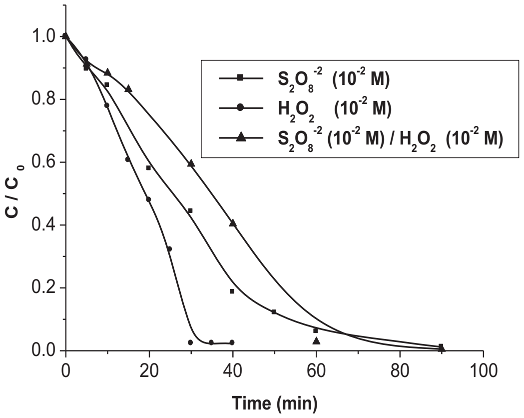

Fig. 13. Comparison of AY (1.6×10^{-4} M) degradation by different processes H_2O_2/UV, $S_2O_8^{2-}$/UV, and $S_2O_8^{2-}/H_2O_2$/UV at same concentration of $S_2O_8^{2-}$ and H_2O_2 (10^{-2} M).

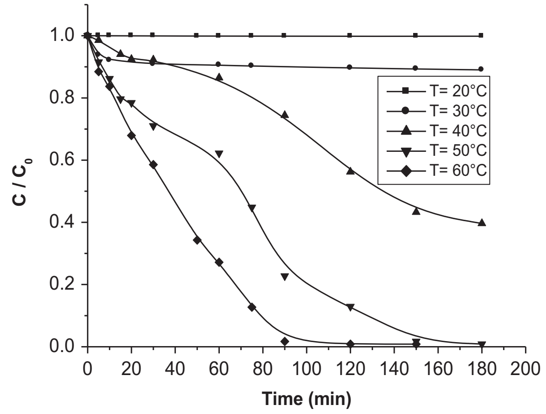

Fig. 14. Effect of temperature on the oxidation of AY (1.6×10^{-4} M) by $S_2O_8^{2-}$ (10^{-2} M) in absence of light, T = 20, 30, 40, 50, 60 ℃.

$$2SO_4^{\cdot -} \rightarrow \text{Chain termination} \qquad k = 3.2 \times 10^8\ \text{M}^{-1}\ \text{s}^{-1} \tag{24}$$

$$\text{Dye} + HO^{\cdot}/SO_4^{\cdot -} \rightarrow \text{Intermediaries} \rightarrow \text{Mineralization} \tag{25}$$

4. Conclusion

This work illustrates the performance and the comparison of different systems to eliminate AY (1.6×10^{-4} M) from an aqueous and homogeneous medium. Experiments conducted on one side by direct UV photolysis at various wavelengths and in solar light and on the other side by acetone/UV, H_2O_2/UV, $S_2O_8^{2-}$/UV, $S_2O_8^{2-}/H_2O_2$/UV, and $S_2O_8^{2-}$/heat (absence of light) are achieved. Moreover, the bleaching rates of AY are determined according to the optimum conditions as concentrations of hydrogen peroxide, persulfate and acetone, and pH and temperature. In direct UV photolysis, the obtained results show that AY presents a negligible decolorization rate for the used concentration and at the following wavelengths: 310, 254, and 365 nm. The reason is the non-absorbance of light by AY. Similar results are obtained in solar light too. By contrast, a real improvement in the decolorization process is observed in presence of the systems listed above. Indeed, from the experimental results, it is found that the color removal rates follow the ascending order for a reaction time of 40 min: UV (artificial and solar light): negligible < H_2O_2/UV (solar light: only 8%) < acetone/UV (10^{-2} M, 17%) < heat/$S_2O_8^{2-}$ (10^{-2} M, 53.65%) < $S_2O_8^{2-}/H_2O_2$/UV (10^{-2} M, and 60%) < $S_2O_8^{2-}$/UV (10^{-2} M, 81.37%) < H_2O_2/UV (10^{-2} M, 97.68%). However, before any treatment, no sensitivity is detected when AY is mixed separately with H_2O_2, $S_2O_8^{2-}$ and acetone for the used concentration. Additionally, in $S_2O_8^{2-}$/UV, when pH is acidic, the major radical is $SO_4^{\cdot -}$ leading to a slight decrease in the decolorization process. Concerning the system $S_2O_8^{2-}/H_2O_2$/UV, we observed that the efficiency decreased slightly. In another side, it should be mentioned that in the absence of light, persulfate is activated at elevated temperatures to produce the radical $SO_4^{\cdot -}$, giving a rapid decolorization of the substrate for the highest temperature and for a reaction time of 100 min. For some concentrations, the depletion of AY is best represented by a pseudo-first-order kinetics for acetone/UV, H_2O_2/UV, and $S_2O_8^{2-}$/UV.

References

[1] A. El-Ghenymy, F. Centellas, J.A. Garrido, R.M. Rodríguez, I. Sirés, P.L. Cabot, E. Brillas, Decolorization and mineralization of Orange G azo dye solutions by anodic oxidation with a boron-doped diamond anode in divided and undivided tank reactors, Electrochim. Acta 130 (2014) 568–576.

[2] L. Das, S. Chatterjee, D.B. Naik, S. Adhikari, Role of surfactant derived intermediates in the efficacy and mechanism for radiation chemical degradation of a hydrophobic azo dye, 1-phenylazo-2-naphthol, J. Hazard. Mater. 298 (2015) 19–27.

[3] Y. Peng, D. Fu, R. Liu, F. Zhang, X. Liang, $NaNO_2$/$FeCl_3$ catalyzed wet oxidation of the azo dye Acid Orange 7, Chemosphere 71 (2008) 990–997.

[4] K.C. Chen, J.Y. Wu, C.C. Huang, Y.M. Liang, S.C.J. Hwang, Decolorization of azo dye using PVA-immobilized microorganisms, J. Biotechnol. 101 (2003) 241–252.

[5] A. Thiam, I. Sirés, J.A. Garrido, R.M. Rodríguez, E. Brillas, Effect of anions on electrochemical degradation of azo dye Carmoisine (Acid Red 14) using a BDD anode and air-diffusion cathode, Sep. Purif. Technol. 140 (2015) 43–52.

[6] A. Thiam, I. Sirés, E. Brillas, Treatment of a mixture of food color additives (E122, E124 and E129) in different water matrices by UVA and solar photoelectro-Fenton, Water Res. 81 (2015) 178–187.
[7] O. Dusart, D. Marmier-Dussoubs, B. Serpaud, Removal of industrial dyes on peat, sawdust, graft cellulose and charcoal, La tribune de l'eau. 44 (1991) 15–22.
[8] F. Perineau, J. Molinier, A. Gaset, Adsorption of ionic dyes on wool carbonizing waste, Water Res. 17 (1983) 559–567.
[9] A. Azam, A. Hamid, Effects of gap size and UV dosage on decolorization of C.I. Acid Orange 7 by UV/H_2O_2 process, J. Hazard. Mater. 133 (2006) 167–171.
[10] J. García-Montaño, X. Domènech, J.A. García-Hortal, F. Torrades, J. Peral, The testing of several biological and chemical coupled treatments for Cibacron Red FN-R azo dye removal, J. Hazard. Mater. 154 (2008) 484–490.
[11] C.H. Wu, Adsorption of reactive dye onto carbon nanotubes: Equilibrium, kinetics and thermodynamics, J. Hazard. Mater. 144 (2007) 93–100.
[12] T. Kurbus, Y.M. Slokar, A.M.L. Le Marechal, The study of the effects of the variables on H_2O_2/UV decoloration of vinylsulphone dye: Part II, Dyes Pigm. 54 (2002) 67–78.
[13] H.Y. Shu, M.C. Chang, H.J. Fan, Decolorization of azo dye acid black 1 by the UV/H_2O_2 process and optimization of operating parameters, J. Hazard. Mater. 113 (2004) 201–208.
[14] D. Salari, A. Niaei, S. Aber, M.H. Rasoulifard, The photooxidative destruction of C.I. Basic Yellow 2 using UV/$S_2O_{82}^-$ process in a rectangular continuous photoreactor, J. Hazard. Mater. 166 (2009) 61–66.
[15] A. Tsitonaki, B. Petri, M. Crimi, H. Mosbæk, R.L. Siegrist, P.L. Bjerg, In situ chemical oxidation of contaminated soil and groundwater using persulfate: A review, Crit. Rev., Environ. Sci. Technol. 40 (2010) 55–91.
[16] G.V. Buxton, C.L. Greenstock, W.P. Helman, A.B. Ross, Critical review of rate constants for reactions of hydrated electrons, hydrogen atoms and hydroxyl radicals ($\cdot OH/\cdot O^-$) in aqueous solution, J. Phys. Chem. 17 (1988) 513–886.
[17] C. Tan, N. Gao, Y. Deng, Y. Zhang, M. Sui, J. Deng, S. Zhou, Degradation of antipyrine by UV, UV/H_2O_2 and UV/PS, J. Hazard. Mater. 260 (2013) 1008–1016.
[18] J.A. Khan, X. He, N.S. Shah, H.M. Khan, E. Hapeshi, D.F. Fatta-Kassinos, D.D. Dionysiou, Kinetic and mechanism investigation on the photochemical degradation of atrazine with activated H_2O_2, $S_2O_8^{2-}$ and HSO_5^-, Chem. Eng. J. 252 (2014) 393–403.
[19] K. Djebbar, S. Aliouche, H. Chenini, T. Sehili, Decolourization process of an azoïque dye (Congo red) by photochemical methods in homogenous medium, Desalination 247 (2009) 412–422.
[20] S. Fassi, K. Djebbar, I. Bousnoubra, H. Chenini, T. Sehili, Oxidation of bromocresol green by different advanced oxidation processes: Fenton, Fenton-like, photo-Fenton, photo-Fenton-like and solar light. Comparative study, Desalin. Water Treat. 52 (2014) 4982–4989.
[21] C.C. Lin, M.S. Wu, Degradation of ciprofloxacin by UV/$S_2O8_2^-$ process in a large photoreactor, J. Photochem. Photobiol., A 285 (2014) 1–6.
[22] S. Fassi, I. Bousnoubra, T. Sehili, K. Djebbar, Degradation of "Bromocresol Green" by direct UV photolysis, acetone/UV and advanced oxidation processes (AOP's) in homogeneous solution (H_2O_2/UV, $S_2O_8^{2-}$/UV). Comparative study, J. Mater. Environ. Sci. 3 (2012) 732–743.
[23] W. Chu, S.M. Tsui, Photo-sensitization of diazo disperse dye in aqueous acetone, Chemosphere 39 (1999) 1667–1677.
[24] F. Banat, S. Al-Asheh, M. Al-Rawashdeh, M. Nusair, Photodegradation of methylene blue dye by the UV/H_2O_2 and UV/acetone oxidation processes, Desalination 181 (2005) 225–232.
[25] S. Yang, P. Wang, X. Yang, L. Shan, W. Zhang, X. Shao, R. Niu, Degradation efficiencies of azo dye Acid Orange 7 by the interaction of heat, UV and anions with common oxidants: Persulfate, peroxymonosulfate and hydrogen peroxide, J. Hazard. Mater. 179 (2010) 552–558.
[26] A. Aleboyeh, Y. Moussa, H. Aleboyeh, Kinetics of oxidative decolourisation of Acid Orange 7 in water by ultraviolet radiation in the presence of hydrogen peroxide, Sep. Purif. Technol. 43 (2005) 143–148.
[27] M.A. Behnajady, N. Modirshahla, M. Shokri, Photodestruction of Acid Orange 7 (AO7) in aqueous solutions by UV/H_2O_2: Influence of operational parameters, Chemosphere 55 (2004) 129–134.
[28] C. Galindo, P. Jacques, A. Kalt, Photochemical and photocatalytic degradation of an indigoid dye: A case study of acid blue 74 (AB74), J. Photochem. Photobiol., A 141 (2001) 47–56.
[29] J.H. Sun, S.P. Sun, G.L. Wang, L.P. Qiao, Degradation of azo dye Amido black 10B in aqueous solution by Fenton oxidation process, Dyes Pigm. 74 (2007) 647–652.
[30] C.S. Liu, C.P. Higgins, F. Wang, K. Shih, Effect of temperature on oxidative transformation of perfluorooctanoic acid (PFOA) by persulfate activation in water, Sep. Purif. Technol. 91 (2012) 46–51.
[31] J. Saien, A.R. Soleymani, J.H. Sun, Parametric optimization of individual and hybridized AOPs of Fe^{2+}/H_2O_2 and UV/$S_2O8_2^-$ for rapid dye destruction in aqueous media, Desalination 279 (2011) 298–305.
[32] R.H. Waldemer, P.G. Tratnyek, R.L. Johnson, J.T. Nurmi, Oxidation of chlorinated ethenes by heat-activated persulfate: Kinetics and products, Environmental Science & Technology 41 (2007) 1010–1015.
[33] K.C. Huang, Z.Q. Zhao, G.E. Hoag, A. Dahmani, P.A. Block, Degradation of volatile organic compounds with thermally activated persulfate oxidation, Chemosphere 61 (2005) 551–560.
[34] S.Y. Oh, H.W. Kim, J.M. Park, H.S. Park, C. Yoon, Oxidation of polyvinyl alcohol by persulfate activated with heat, Fe^{2+}, and zero-valent iron, J. Hazard. Mater. 168 (2009) 346–351.
[35] X. He, A.A. de la Cruz, K.E. O'Shea, D.D. Dionysiou, Kinetics and mechanisms of cylindrospermopsin destruction by sulfate radical-based advanced oxidation processes, Water Res. 63 (2014) 168–178.

[36] T.K. Lau, W. Chu, N.J.D. Graham, The aqueous degradation of butylated hydroxyanisole by UV/$S_2O_8^{2-}$: Study of reaction mechanisms via dimerization and mineralization, Environ. Sci. Technol. 41 (2007) 613–619.

[37] K.L. Ivanov, E.M. Glebov, V.F. Plyusnin, Y.V. Ivanov, V.P. Grivin, N.M. Bazhin, Laser flash photolysis of sodium persulfate in aqueous solution with additions of dimethylformamide, J. Photochem. Photobiol., A 133 (2000) 99–104.

[38] K.C. Huang, R.A. Couttenye, G.E. Hoag, Kinetics of heat assisted persulfate oxidation of methyl tert-butyl ether (MTBE), Chemosphere 49 (2002) 413–420.